

Do annuloplasty rings designed to treat ischemic/functional mitral regurgitation alter left-ventricular dimensions in the acutely ischemic ovine heart?



Wolfgang Bothe, MD,^{a,b} John-Peder Escobar Kvitting, MD, PhD,^{b,c} Manuel K. Rausch, PhD,^d Tomasz A. Timek, MD,^{b,e} Julia C. Swanson, MD,^{b,f} David H. Liang, MD, PhD,^g Mario Walther, PhD,^h Ellen Kuhl, PhD,^{b,i} Neil B. Ingels, Jr, PhD,^{b,j} and D. Craig Miller, MD^b

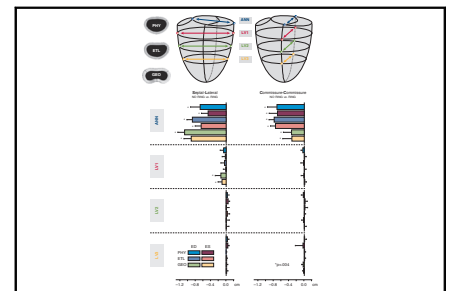
ABSTRACT

Objective: To quantify the effects of annuloplasty rings designed to treat ischemic/functional mitral regurgitation on left ventricular septal-lateral (S-L) and commissure-commissure (C-C) dimensions.

Methods: Radiopaque markers were placed as opposing pairs on the S-L and C-C aspects of the mitral annulus and the basal, equatorial, and apical level of the left ventricle (LV) in 30 sheep. Ten true-sized Carpentier-Edwards Physio (PHY), Edwards IMR ETlogix (ETL), and GeoForm (GEO; all from Edwards Lifesciences, Irvine, Calif) annuloplasty rings were inserted in a releasable fashion. After 90 seconds of left circumflex artery occlusion with the ring implanted (RING), 4-dimensional marker coordinates were obtained using biplane videofluoroscopy. After ring release, another data set was acquired after another 90 seconds of left circumflex artery occlusion (NO RING). S-L and C-C diameters were computed as the distances between the respective marker pairs at end-diastole. Percent change in diameters was calculated between RING versus NO RING as $100 \times (\text{diameter in centimeters [RING]} - \text{diameter in centimeters [NO RING]}) / \text{diameter in centimeters [NO RING]}$.

Results: Compared with NO RING, all ring types (PHY, ETL, and GEO) reduced mitral annular S-L dimensions by $-20.7 \pm 5.6\%$, $-26.8 \pm 3.9\%$, and $-34.5 \pm 3.8\%$, respectively. GEO reduced the S-L dimensions of the LV at the basal level only by $-2.3 \pm 2.4\%$, whereas all other S-L dimensions of the LV remained unchanged with all 3 rings implanted. PHY, ETL, and GEO reduced mitral annular C-C dimensions by $-17.5 \pm 4.8\%$, -19.6 ± 2.5 , and $-8.3 \pm 4.9\%$, respectively, but none of the rings altered the C-C dimensions of the LV.

Conclusions: Despite radical reduction of mitral annular size, disease-specific ischemic/functional mitral regurgitation annuloplasty rings do not induce relevant changes of left ventricular dimensions in the acutely ischemic ovine heart. (J Thorac Cardiovasc Surg 2019;158:1058-68)



Mean differences in diameters between NO RING versus RING at end-diastole/systole.

Central Message

Despite radical reduction of mitral annular size, disease-specific IMR/FMR annuloplasty rings do not induce relevant changes of left ventricular dimensions in the acutely ischemic ovine heart.

Perspective

The disproportionate septal-lateral downsizing of annuloplasty rings to treat IMR/FMR is intended to maximize leaflet coaptation and reshape the dilated, spherical left ventricle. If the findings from this acute ischemic preparation do translate to patients, implantation of an etiology-specific designed ring alone might not be sufficient to acutely restore the ventricle to its normal elliptical shape.

See Commentaries on pages 1069 and 1071.

From the ^aDepartment of Cardiovascular Surgery, Heart Center Freiburg - Bad Krozingen, Faculty of Medicine, University of Freiburg, Germany; Departments of ^bCardiothoracic Surgery and ^cCardiology, Stanford University School of Medicine, Stanford, Calif; ^dDepartment of Cardiothoracic Surgery, Oslo University Hospital, Rikshospitalet, Oslo, Norway; ^eAerospace Engineering & Engineering Mechanics, University of Texas at Austin, Austin, Tex; ^fDivision of Cardiothoracic Surgery, Spectrum Health, Grand Rapids, Mich; ^gProvidence Heart and Vascular Institute, Providence St Vincent Hospital, Portland, Ore; ^hDepartment of Mathematics and Applied Statistics, University of Applied Sciences, Jena, Germany; ⁱDepartment of Mechanical Engineering, Stanford University School of Engineering, Stanford, Calif; and ^jLaboratory of Cardiovascular Physiology and Biophysics, Research Institute of the Palo Alto Medical Foundation, Palo Alto, Calif.

D. Craig Miller received R01 research grants from the National Heart, Lung, and Blood Institute, National Institutes of Health: HL29589 (1982-2008) and HL67025 (2001-2010).

Received for publication April 4, 2018; revisions received Dec 19, 2018; accepted for publication Dec 21, 2018.

Address for reprints: D. Craig Miller, MD, Department of Cardiothoracic Surgery, Falk Cardiovascular Research Center, Stanford University School of Medicine, Stanford, CA 94305-5407 (E-mail: dcm@stanford.edu).

0022-5223/\$36.00

Copyright © 2019 Published by Elsevier Inc. on behalf of The American Association for Thoracic Surgery

<https://doi.org/10.1016/j.jtcvs.2018.12.077>

Abbreviations and Acronyms

ANN	= mitral valve annulus
APM	= anterolateral papillary muscle
C-C	= commissure-commissure
ED	= end-diastole
ES	= end-systole
ETL	= Edwards IMR ETlogix annuloplasty ring
FMR	= functional mitral regurgitation
GEO	= Edwards GeoForm annuloplasty ring
IMR	= ischemic mitral regurgitation
LCx	= left circumflex artery
LV	= left ventricle
LV1	= basal level of the left ventricle
LV2	= equatorial level of the left ventricle
LV3	= apical level of the left ventricle
NO RING	= data obtained under ischemic conditions after ring release
PHY	= Carpentier-Edwards Physio
PPM	= posteromedial papillary muscle
RING	= data obtained under ischemic conditions with ring implanted
S-L	= septal-lateral



Scanning this QR code will take you to the article title page to access supplementary information.



During left ventricular remodeling after acute myocardial infarction, the normal elliptical shape of the left ventricle (LV) might become more spherical¹ resulting in papillary muscle displacement, leaflet tethering, malcoaptation, and mitral regurgitation.² These changes, if not attenuated or reversed by intervention, are associated with a poor clinical prognosis.³

The implantation of an undersized annuloplasty ring represents the contemporary standard surgical approach for treating ischemic mitral regurgitation (IMR)/functional mitral regurgitation (FMR), but this procedure is associated with suboptimal clinical results due to ongoing LV remodeling and recurrent leaflet tethering/malcoaptation.⁴ Under the assumption that the spherical geometry of the LV might be altered by a mitral annular intervention, disease-specific IMR/FMR annuloplasty rings (Edwards IMR ETlogix [ETL] and Edwards GeoForm [GEO]; Edwards Lifesciences, Irvine, Calif) have been introduced in clinical practice. These annuloplasty rings include a disproportionate

downsizing of the septal-lateral (S-L) dimension,⁵ thereby aiming to improve leaflet coaptation and—potentially—to restore a more elliptical shape of the LV.⁶ Furthermore, in the GEO ring, the mid-lateral mitral annular segment (Figure 1, A, P2) is elevated by approximately 5 mm to lift up the displaced posteromedial papillary muscle (PPM).⁷

Clinically, implantation of IMR/FMR rings has been associated with reverse LV remodeling, restoration of LV geometry, and reduced leaflet tethering.⁸ Such changes have, however, also been reported with conventional rings^{9,10} and it is currently unknown whether these geometrical alterations are: (1) due to a postoperative myocardial recovery (eg, caused by better myocardial perfusion after coronary artery bypass surgery) eventually leading to LV reverse remodeling; or (2) an immediate, annuloplasty ring-related effect on the geometry of the LV. We hypothesized that disease-specific IMR/FMR rings reduce left ventricular S-L, but not commissure-commissure (C-C) dimensions and that the GEO ring lifts up the PPM during acute ovine posterolateral ischemia.

METHODS**Surgical Preparation**

These data, including the experimental methods, have been in part, previously published.^{11–15} In brief, 30 adult male sheep (49 ± 4 kg) were premedicated with ketamine (25 mg/kg intramuscularly), anesthetized with sodium thiopental (6.8 mg/kg intravenously), intubated, and mechanically ventilated with inhalational isoflurane (1.0%–2.5%). All animals received humane care in compliance with the *Principles of Laboratory Animal Care* formulated by the National Society of Medical Research and the *Guide for Care and Use of Laboratory Animals* prepared by the National Academy of Sciences and published by the National Institute of Health (DHEW NIH publication 85-23, revised 1985). This study was approved by the Stanford Medical Center Laboratory Research Animal Review committee and conducted according to Stanford University policy.

Through a left thoracotomy, 12 radiopaque markers were implanted to silhouette the LV at the cross-section points of 4 equally spaced longitudinal and 3 transverse meridians and 1 on the LV apex (Figure 1). Using cardiopulmonary bypass and cardioplegic arrest, 8 radiopaque markers were implanted equidistantly along the mitral annulus, with 1 marker sewn on the anterolateral papillary muscle (APM) and 1 on the PPM tip. Three different annuloplasty ring types were implanted (1 ring per animal), 1 conventional (Carpentier-Edwards Physio [PHY], Edwards Lifesciences) and 2 etiology-specific (ETL and GEO; both from Edwards Lifesciences). To allow each animal to serve as its own control, annuloplasty rings were implanted in a releasable fashion as previously described. In brief, the annuloplasty rings were prepared before the operation in the following manner: the middle parts of 8 double-armed polyester braided sutures were stitched evenly spaced around the ring from the bottom to the top side using a “spring eye” needle. The resulting loops were “locked” with 2 polypropylene sutures. The polyester sutures were stitched equidistantly in a perpendicular direction from the ventricular to the atrial side through the mitral annulus. The annuloplasty devices were secured to the mitral annulus by tying these sutures. The locking sutures (polypropylene) and the drawstrings were exteriorized before the atrium was closed (see Bax and colleagues¹¹ for details). All operations were performed by 2 experienced cardiac surgeons (W.B. and J.-P.E.K.). All prostheses were “true-sized” by assessing height and entire area of the anterior mitral leaflet,

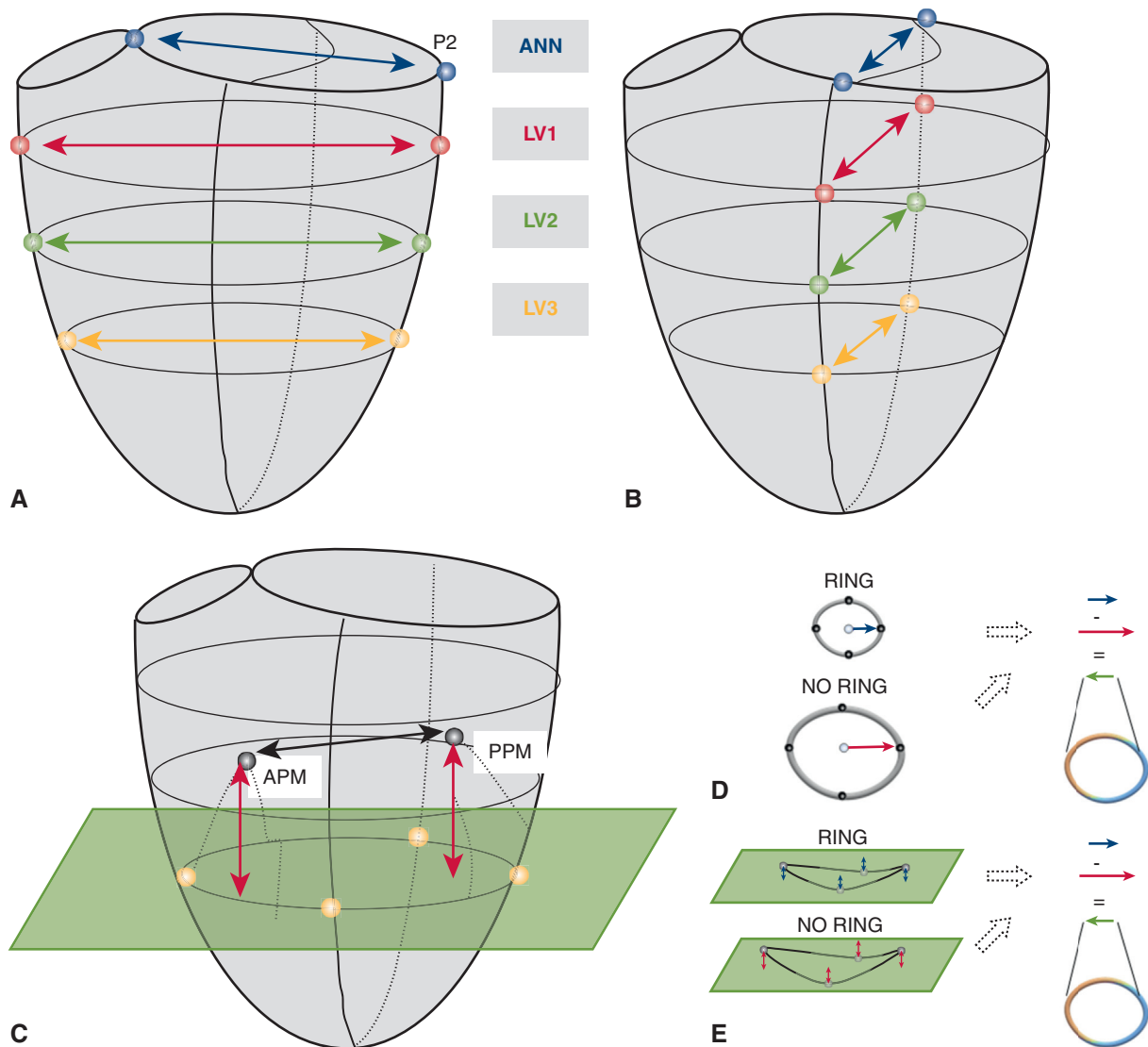


FIGURE 1. Septal-lateral (A) and commissure-commissure (B) diameters were calculated from the respective marker pairs on the mitral annulus (ANN) and the basal (LV1), equatorial (LV2), and apical (LV3) levels of the left ventricle. To assess whether the implanted rings lift up the papillary muscle tips, the orthogonal distances of anterolateral and posteromedial papillary muscle (APM and PPM, respectively) markers to a least-squares reference plane were calculated (red arrows, C). Interpapillary muscle distance was calculated as distance in 3-D space between APM and PPM tip (black arrow, C). D, To calculate continuous transverse changes along the ANN and LV1, LV2, and LV3 transverse left ventricular meridians before and after ring implantation, we used a least-squares approach to position the knot locations in such a fashion that the distance between the fiduciary marker coordinates and the spline were minimized. We chose the number of knots equal to the number of fiduciary markers with equal weights. Next, we computed the distance vectors between all points on the splines and the centers of their respective spline fits (before and after ring implantation), and projected these vectors onto their splines' best-fit plane. Finally, we subtracted those transverse distance values with ring implanted (RING) from the same values after ring release (NO RING). E, Continuous height profile was defined as the best-fit spline through the fiduciary markers from their best fit plane. To calculate continuous height profile changes, we used the same spline representations of annulus/transverse meridians and again calculated their best fit planes. Then, we determined the orthogonal distance of all points along the annulus/transverse meridians from the best fit plane and subtracted those values without ring implantation from those with ring implantation (RING – NO RING; E). We repeated this procedure for all ring types and their respective controls for end-diastole and end-systole. The schematics (D) and (E) show 4 markers (ie, representing the calculations for LV1-3). Note that 8 markers were used for the calculations (transverse changes and height profile) of the mitral annulus. P2, Mid-lateral mitral annular marker.

and all received a size 28-mm ring. The left circumflex artery (LCx) was then encircled immediately distal to the first obtuse marginal branch with a vessel loop. The animals, while intubated and anesthetized, were then transferred with the chest open to the experimental catheterization laboratory.

Data Acquisition

Videofluoroscopic images (60 frames per second) of all radiopaque markers were acquired using biplane videofluoroscopy (Philips Medical Systems, North America, Pleasanton, Calif). Acute left ventricular

ischemia was induced by tightening the LCx vessel loop for 90 seconds, and a data set under ischemic conditions with ring was obtained (RING). After hemodynamic values returned to baseline (determined by hemodynamic values return to normal) and myocardial contraction (no regional wall motion abnormalities in the echocardiography) after release of the LCx vessel loop, the ring was released from the mitral annulus by removing the “locking sutures” (discussed previously) and pulling the ring to the roof of the left atrium using the drawstring sutures.¹¹ Another data acquisition was performed with the ring released and reocclusion of the LCx for 90 seconds (NO RING).

Marker coordinates from 3 consecutive sinus rhythm beats from each of the biplane views were then digitized and merged to yield the time-resolved 3-D coordinates of each marker centroid in each frame using semiautomated image processing and digitization software.^{16,17} Electrocardiogram and analogue left ventricular pressures were recorded in real-time on the video images. The degree of mitral regurgitation after each data acquisition run was graded by an independent echocardiographer (D.H.L.) on the basis of color Doppler regurgitant jet extent and width and categorized as none (0), mild (+1), moderate (+2), moderate to severe (+3), or severe (+4), and then—according to the American Society of Echocardiography guidelines¹⁸—sorted into the categories mild, moderate, or severe. Quantitative methods such as effective regurgitant orifice area and quantitative Doppler were not possible because of limited image quality.

Data Analysis

Except from hemodynamics, all data were calculated at end-diastole (ED) and at end-systole (ES). For each beat, ED was defined as the videofluoroscopic frame containing the peak of the R wave on the electrocardiogram and ES as the frame preceding maximum left ventricular dP/dt.

Hemodynamics. Instantaneous left ventricular volume was computed from the epicardial left ventricular markers using a space-filling multiple tetrahedral volume method.^{16,17} Hemodynamic data were calculated from marker-derived instantaneous left ventricular volumes and analogue left ventricular pressures as previously published.¹³

Mitral annular and left ventricular dimensions. S-L and C-C dimensions were computed as distances between the respective marker pairs on the mitral annular (ANN) as well as basal (LV1), equatorial (LV2), and apical (LV3) levels of the LV (Figure 1, A and B). Percent change in measured parameters between RING versus NO RING was calculated as $100 \times ((\text{diameter in centimeters (RING)} - \text{diameter in centimeters (NO RING)}) / \text{diameter in centimeters [NO RING]})$.

Interpapillary muscle distance. Interpapillary muscle distance was calculated as distance in 3-D space between respective papillary muscle tip markers. The distance was calculated at ED and ES.

Distances of APM and PPM to the left ventricular apical plane.

To assess whether the implanted rings—because of their height profile (eg, the mid-lateral mitral annular segment elevation of the GEO ring)—are able to lift up the papillary muscle tips, the orthogonal distances of APM and PPM markers to a least-squares reference plane were calculated at ED and ES. The mitral annular plane is, however, significantly affected by ring implantation and, thus, does not serve as a stable reference plane. A plane generated from the 4 ventricular markers on the LV3 was therefore used under the assumption that the markers with the largest distance to the mitral annulus are least affected by the ring implantation (Figure 1, C).

To simplify the understanding of the effects of ring implantation, differences between RING and NO RING were calculated as distance in centimeters (RING) – distance in centimeters (NO RING). That is, positive/negative values reflect an increase/decrease, respectively, induced by ring implantation.

Spline curves showing changes in transverse and longitudinal dimensions of mitral annulus, LV1, LV2, and LV3.

In order to provide a more visual, qualitative description of geometric changes of the LV induced by ring implantation, changes in the transverse and longitudinal dimension of mitral annulus and LV were calculated and displayed on spline curves: to calculate continuous transverse changes along the ANN and the 3 left-ventricular transverse meridians (LV1, LV2, LV3) before and after ring implantation, we used a least-squares approach to position the knot locations in such a fashion that the distance between the fiducial marker coordinates and the spline were minimized. We chose the number of knots equal to the number of fiducial markers with equal weights. Next, we computed the distance vectors between all points on the splines and the centers of their respective spline fits (before and after ring implantation), and projected these vectors onto their splines' best-fit plane. Finally, we subtracted those transverse distance values after ring release (NO RING; Figure 1, D) from the same values with ring implanted (RING). We computed cubic spline curves during occlusion for RING and NO RING. We did not center the 2 conditions, but instead compared the distances with the respective centers.

Continuous height profile was defined as the best-fit spline through the fiducial markers from their best fit plane. To calculate continuous height profile changes, we used the same spline representations of annulus/transverse meridians and again calculated their best fit planes. Then, we determined the orthogonal distance of all points along the annulus/transverse meridians from the best fit plane and subtracted those values without ring implantation from those with ring implantation (RING – NO RING; Figure 1, E). We repeated this procedure for all ring types and their respective controls for ED and ES.

Statistical analysis. As previously mentioned, the presented data are a secondary analysis from data sets that have in part been

TABLE 1. Hemodynamic data

	PHY			ETL			GEO		
	NO RING	RING	P value	NO RING	RING	P value	NO RING	RING	P value
Mitral regurgitation grade	1.0 (1.0-2.0)	0.5 (0.0-0.5)	<.004	0.5 (0.0-3.0)	0.0 (0.0-0.5)	.017	2.0 (1.0-2.0)	0.0 (0.0-0.5)	<.004
HR, per minute	90 ± 11	90 ± 14	.833	82 ± 6	82 ± 7	.648	92 ± 10	93 ± 10	.490
LVEDV, mL	133 ± 34	135 ± 36	.068	130 ± 23	131 ± 22	.389	122 ± 17	121 ± 16	.596
dP/dt _{max} , mm Hg/s	1005 ± 231	1077 ± 225	.130	921 ± 294	923 ± 239	.977	1012 ± 242	1085 ± 231	.060
LVP _{max} , mm Hg	71 ± 7	75 ± 9	.460	72 ± 9	74 ± 7	.3374	74 ± 7	76 ± 6	.437

Results for mitral regurgitation grade is represented as median with interquartile range and the remaining hemodynamic data are presented as mean ± 1 standard deviation; P values for mitral regurgitation grade are on the basis of a Wilcoxon rank sum test and for the remaining hemodynamic data paired *t* test. Bonferroni adjusted level of significance $P < .017$. PHY, Physio annuloplasty ring (Edwards Lifesciences, Irvine, Calif); ETL, IMR ETlogix annuloplasty ring (Edwards Lifesciences); GEO, GeoForm annuloplasty ring (Edwards Lifesciences); mitral regurgitation, mitral regurgitation; HR, heart rate; LVEDV, left ventricular end-diastolic volume; dP/dt_{max}, maximal rate of rise of left ventricular pressure; LVP_{max}, maximum left ventricular pressure.

TABLE 2. Mitral annular and left ventricular diameters

	S-L							
	ED				ES			
	NO RING	RING	Percent change*	P value	NO RING	RING	Percent change*	P value
ANN								
PHY	3.17 ± 0.37	2.50 ± 0.15	−20.7 ± 5.6	<.001	2.97 ± 0.31	2.50 ± 0.16	−15.4 ± 4.1	<.001
ETL	3.26 ± 0.18	2.38 ± 0.17	−26.8 ± 3.9	<.001	3.03 ± 0.20	2.38 ± 0.16	−21.2 ± 4.4	<.001
GEO	3.10 ± 0.21	2.02 ± 0.09	−34.5 ± 3.8	<.001	2.95 ± 0.23	2.05 ± 0.09	−30.4 ± 4.4	<.001
LV1								
PHY	5.81 ± 0.48	5.75 ± 0.42	−0.96 ± 1.5	.116	5.67 ± 0.33	5.65 ± 0.27	−0.30 ± 1.4	.537
ETL	6.07 ± 0.42	6.03 ± 0.44	−0.71 ± 1.5	.263	5.83 ± 0.34	5.83 ± 0.34	−0.04 ± 1.14	.938
GEO	5.93 ± 0.26	5.79 ± 0.22	−2.26 ± 2.4	.001*	5.62 ± 0.24	5.52 ± 0.21	−1.84 ± 1.9	.001
LV2								
PHY	5.23 ± 0.65	5.26 ± 0.63	0.71 ± 1.4	.431	4.91 ± 0.58	4.96 ± 0.56	1.14 ± 0.8	.109
ETL	5.16 ± 0.65	5.16 ± 0.59	0.21 ± 2.2	.939	4.78 ± 0.45	4.81 ± 0.42	0.72 ± 1.3	.333
GEO	5.29 ± 0.30	5.29 ± 0.27	0.09 ± 1.5	.940	4.76 ± 0.31	4.77 ± 0.30	0.17 ± 1.4	.839
LV3								
PHY	3.51 ± 0.45	3.54 ± 0.46	0.91 ± 1.2	.352	3.27 ± 0.40	3.31 ± 0.39	1.40 ± 1.1	.175
ETL	3.38 ± 0.60	3.38 ± 0.59	0.03 ± 0.5	.994	3.22 ± 0.49	3.23 ± 0.48	0.40 ± 0.6	.695
GEO	3.60 ± 0.47	3.62 ± 0.48	0.32 ± 0.8	.733	3.43 ± 0.50	3.45 ± 0.52	0.36 ± 1.1	.645

All values are in centimeters, mean ± 1 standard deviation; *P* values are on the basis of a mixed effect model. Bonferroni adjusted level of significance $P < .004$. *S-L*, Septal-lateral; *C-C*, commissure-commissure; *ED*, end-diastole; *ES*, end-systole; *ANN*, mitral annulus; *PHY*, Physio annuloplasty ring (Edwards Lifesciences, Irvine, Calif); *ETL*, IMR ETlogix annuloplasty ring (Edwards Lifesciences); *GEO*, GeoForm annuloplasty ring (Edwards Lifesciences); *LV1*, basal level of the left ventricle; *LV2*, equatorial level of the left ventricle; *LV3*, apical level of the left ventricle. *NO RING versus RING.

previously published. The sample size was initially determined to assess differences in mitral annular and leaflet strains with and without 5 different annuloplasty ring types using SamplePower 2.0 (SPSS, Inc, Chicago, Ill). Data are reported as mean ± 1 standard deviation unless otherwise stated. Hemodynamic data were analyzed using paired *t* test except for the grading of mitral regurgitation for which the nonparametric Wilcoxon rank sum test was applied. For the statistical analysis of ring effects (RING vs NO RING) on S-L/C-C diameters and distances (interpapillary muscle distance, distance of APM and PPM to the LV apical plane) we used a mixed effect model approach to account for inter-related measurements within the sheep. For each of the measurement conditions (ED and ES) as well as their combination with S-L and C-C for the diameter data we applied a separate mixed effect model. In each model we included presence of ring (RING or NO RING), ring type (PHY, ETL, GEO), and location (ANN, LV1, LV2, LV3) for the diameter (S-L/C-C) and distance data (interpapillary muscle distance, distance of APM and PPM to the LV apical plane) as fixed factors together with their interactions into the model. To account for inter-relation and for different variation (which could be shown in an explorative data analysis) we incorporated a ring type-specific random intercept as well as a location-specific (for the diameter data) and muscle-specific (for the distance data) random effect. The level of significance was set at 5%. For each statistical analysis we reported the nominal *P* values, which were the basis for the Bonferroni adjustments: (1) for the hemodynamic data we adjusted each parameter separately with respect to the 3 ring types (PHY, ETL, and GEO; ie, the Bonferroni adjusted level of significance was set to 0.05/3; (2) for mitral annular and left ventricular diameters the adjustment was made separately for each combination of diameters (C-C, S-L) and measurement conditions (ED, ES) on the basis of the 4 location (ANN, LV1, LV2, LV3) and the 3 ring types (ie, the Bonferroni-adjusted level of significance was set to 0.05/12; (3) for distances of APM and PPM to the LV apical plane the adjustment was on the basis of the 2 different papillary muscles (APM and PPM) and the 3 ring types, so the Bonferroni-adjusted level of significance was set to

0.05/6. All analyses were performed using SAS version 9.4 (SAS Institute Inc, Cary, NC).

RESULTS

Hemodynamics

Table 1 shows a summary of the hemodynamic data. No differences between RING versus NO RING with respect to heart rate, left ventricular end-diastolic volume, maximal rate of rise of left ventricular pressure (dP/dt_{max}), or maximum left ventricular pressure were observed. All 3 rings effectively prevented mitral regurgitation during acute left ventricular ischemia.

Mitral Annular and Left Ventricular Dimensions

Table 2 shows mitral annular as well as left ventricular S-L and C-C diameters at ED and at ES. Figure 2, A illustrates differences in S-L and C-C diameters between NO RING versus RING state at ED and at ES. At both time points all ring types (PHY, ETL, and GEO) significantly reduced mitral annular S-L dimensions (ED: $-20.7 \pm 5.6\%$, $-26.8 \pm 3.9\%$, and $-34.5 \pm 3.8\%$, ES: $-15.4 \pm 4.12\%$, $-21.2 \pm 4.4\%$, and $-30.4 \pm 4.4\%$, respectively) compared with NO RING. GEO reduced the S-L dimension of the LV at the basal level (LV1) by $-2.3 \pm 2.4\%$ and $-1.8 \pm 1.9\%$ at ED and ES, respectively, whereas all other S-L dimensions of the LV were not affected by any of the implanted ring types. PHY, ETL, and GEO reduced mitral annular C-C dimensions (ED: $-17.5 \pm 4.8\%$, $-19.6 \pm 2.5\%$, and $-8.3 \pm 4.9\%$; ES:

TABLE 2. Continued

C-C							
ED				ES			
NO RING	RING	Percent change*	P value	NO RING	RING	Percent change*	P value
4.01 ± 0.31	3.30 ± 0.09	−17.5 ± 4.8	<.001	4.00 ± 0.27	3.30 ± 0.08	−17.3 ± 4.3	<.001
4.00 ± 0.23	3.21 ± 0.15	−19.6 ± 2.5	<.001	3.96 ± 0.24	3.21 ± 0.16	−19.0 ± 2.4	<.001
3.87 ± 0.25	3.54 ± 0.09	−8.35 ± 4.9	<.001	3.83 ± 0.31	3.54 ± 0.09	−7.18 ± 6.1	<.001
7.04 ± 0.63	7.00 ± 0.64	−0.58 ± 0.7	.266	6.51 ± 0.53	6.52 ± 0.55	0.13 ± 0.7	.793
7.48 ± 0.37	7.46 ± 0.36	−0.21 ± 1.	.656	6.86 ± 0.41	6.86 ± 0.42	0.07 ± 0.7	.886
6.76 ± 0.35	6.75 ± 0.31	−0.10 ± 1.1	.803	6.37 ± 0.33	6.38 ± 0.33	0.24 ± 0.7	.698
6.84 ± 0.41	6.81 ± 0.39	−0.36 ± 0.8	.494	6.02 ± 0.45	6.04 ± 0.43	0.32 ± 1.0	.671
6.98 ± 0.28	6.99 ± 0.25	0.26 ± 0.9	.632	6.10 ± 0.36	6.10 ± 0.35	0.08 ± 0.5	.909
6.64 ± 0.43	6.62 ± 0.43	−0.46 ± 0.6	.542	5.95 ± 0.38	5.95 ± 0.36	−0.01 ± 0.7	.913
3.63 ± 0.59	3.65 ± 0.57	0.40 ± 1.3	.748	3.27 ± 0.54	3.23 ± 0.47	−0.58 ± 5.3	.404
4.18 ± 0.63	4.19 ± 0.65	0.15 ± 0.6	.821	3.71 ± 0.53	3.72 ± 0.54	0.20 ± 0.8	.828
3.93 ± 0.29	3.90 ± 0.30	−0.78 ± 0.9	.392	3.41 ± 0.40	3.39 ± 0.39	−0.48 ± 0.8	.663

−17.3 ± 4.3%, −19.0 ± 2.4%, and −7.2 ± 6.1%, respectively), whereas left ventricular C-C dimensions remained unchanged with any of the implanted ring types.

Interpapillary Muscle Distance

Interpapillary muscle distances were not altered by ring implantation either at ED or at ES for PHY (NO RING vs RING, ED: 3.19 ± 0.31 vs 3.21 ± 0.31 cm, $P = .584$; ES: 2.63 ± 0.39 vs 2.67 ± 0.39 cm, $P = .080$), ETL (NO RING vs RING, ED: 3.59 ± 0.23 vs 3.61 ± 0.24 cm, $P = .424$; ES: 3.01 ± 0.22 vs 3.04 ± 0.24 cm, $P = .347$) or GEO (NO RING vs RING, ED: 3.17 ± 0.24 vs 3.18 ± 0.25 cm, $P = .823$; ES: 2.72 ± 0.26 vs 2.75 ± 0.27 cm, $P = .183$).

Distances of APM and PPM to the Left Ventricular Apical Plane

Table 3 and Figure 2, B show the distances and mean differences in distances, respectively, of the APM and PPM to the left ventricular apical plane. APM and PPM distances to the left ventricular apical plane were not altered by ring implantation.

Spline Curves Showing Transverse and Longitudinal Changes of Mitral Annulus, LV1, LV2, and LV3

Figures 3 and 4 show marker-derived spline curves of the ANN as well as the 3 transverse meridians (LV1, LV2, LV3) showing continuous transverse and longitudinal changes, respectively, at ED and ES for PHY, ETL, and GEO rings.

Although ring-induced alterations in the transverse and longitudinal directions were observed on the annular level (ANN), no significant changes were seen on any of the ventricular levels (LV1, LV2 or LV3).

DISCUSSION

Compared with the ischemic heart without ring, the key findings of this in vivo ovine study were that: (1) all annuloplasty ring types (PHY, ETL, and GEO) significantly reduced mitral annular S-L and C-C dimensions, but—except from a small reduction with GEO on the basal ventricular level (LV1) in the S-L dimension (−2.3 ± 2.4% and −1.8 ± 1.9% at ED and ES, respectively)—no significant changes of left ventricular S-L and C-C dimensions were induced; (2) interpapillary muscle distances were not reduced by any ring type (PHY, ETL, and GEO) used; and (3) none of the rings altered the distance of the APM or PPM tip to the left ventricular apical plane during acute posterolateral ischemia. The key findings of this study are illustrated in Video 1.

A reduction of left ventricular diameters after annuloplasty ring implantation in patients with IMR/FMR has been observed for conventional and disease-specific ring types.⁸⁻¹⁰ It is unclear whether the observed changes are caused by improved myocardial perfusion (after concomitant coronary artery bypass surgery) or immediate, annuloplasty-related effects on the geometry of the LV. Although immediate effects of mitral annular downsizing on the curvature of the LV have been observed in the experimental setting,¹⁹ the effects of annuloplasty

rings on the geometry of the ventricle is unclear. This is particularly true for annuloplasty rings specifically designed to address the pathophysiologic alterations of the LV during IMR/FMR. These prostheses (GEO and ETL) incorporate a disproportionate downsizing of the S-L dimension in their design compared with the PHY ring.⁵ In our analysis, the GEO ring reduced the S-L diameter by approximately 35% during acute ischemia, yet despite such radical downsizing of the annular S-L dimension, the reduction of the left ventricular S-L dimension was only approximately 2%. Assuming a 60-mm left-ventricular end-diastolic diameter in a patient with heart failure, the degree of ventricular S-L reduction that could be expected by implantation of the GEO ring would be 1.2 mm. Such magnitude of left ventricular S-L reduction appears too small to effectively restore a more elliptical LV shape. Consequently, the observed reduction of left ventricular diameters after annuloplasty ring implantation in patients with IMR/FMR is most probably due to restored valve competence or improved myocardial perfusion and contractility.

We did not observe any ring effects on the position of APM or PPM. This was true for the distance to the left ventricular apical plane and the interpapillary muscle distances. It therefore appears reasonable to conclude that disease-specific IMR/FMR rings are not effective in repositioning displaced papillary muscles and thus decreasing tethering forces in patients with IMR/FMR.

In this study we qualitatively analyzed changes in height profiles of the 3 left ventricular meridians induced by the implantation of IMR/FMR specific annuloplasty rings. Although relevant changes in the mitral annular height profile can be observed, ring implantation did not affect the height profile of the left ventricular meridians (LV1, LV2, or LV3; Figure 4). These data suggest that the geometry of the LV cannot be altered in the longitudinal direction by interventional changes of the mitral annular height profile.

The surgical repair of IMR/FMR remains challenging. Early clinical data appeared promising in small patient cohorts,^{9,20} but in a recent multicenter randomized study of IMR patients, addressing the mitral annulus alone with a reductive ring annuloplasty was associated with almost 60% recurrent insufficiency rates at a 2-year follow-up.⁴ It is unclear whether disease-specific IMR/FMR rings have the potential to improve these outcomes, and only sporadic clinical data have been reported.^{6,8,21-28} Timek and colleagues reported freedom from recurrent mitral regurgitation at 5 years of 86% using the GEO in 86 patients with 32 patients remaining at risk.⁸ These results are in sharp contrast to the CTSNET trial (Comparing the Effectiveness of Repairing Versus Replacing the Heart's Mitral Valve in People With Severe Chronic Ischemic Mitral Regurgitation, NCT00807040) perhaps driven by differences in inclusion criteria. Compared with the GEO

study, more patients with severe mitral regurgitation were included in the CTSNET trial. The observed improvement could therefore in part be due to patient selection rather than to an effect of the GEO.²⁷

In a retrospective study of 156 patients undergoing implantation of an ETL, preoperative IMR grades were higher (92.3% > grade 2) than in the GEO study. Despite high preoperative IMR grades, Campisi and colleagues reported a freedom from greater than mild regurgitation in 89% of the 156 patients 28 months after surgery.²⁸ These results are promising, but must be validated in larger, prospective studies with longer follow-up. On the basis of our ovine study, we hypothesize that improvements in clinical outcomes are a result of more radical, disproportionate downsizing of the mitral annulus and not subvalvular ring effects on the LV.

Clinical Inferences

If the findings of this study translate to IMR/FMR patients, 2 main inferences may be drawn. First, the left ventricular geometry cannot be effectively altered through a mitral annular intervention using IMR/FMR-specific annuloplasty rings. Consequently, the restoration of a more elliptical left ventricular shape observed weeks/months after annuloplasty in IMR/FMR patients is most probably a result of left ventricular reverse remodeling/myocardial recovery resulting from increased myocardial perfusion and/or restored valve competence. Second, because ring-induced alterations of the mitral annular geometry do not influence papillary muscle tip geometry, IMR/FMR annuloplasty rings might not be effective in relieving tethering forces induced by displaced papillary muscles. Consequently, if potential future trials using disease-specific IMR/FMR rings show a better long-term freedom from recurrent mitral regurgitation compared with conventional, undersized rings, such an improvement in outcomes might be more attributable to the ring-inherent radical, disproportionate S-L mitral annular downsizing rather than to a subvalvular effect of the annuloplasty ring on the LV. If conventional rings are used, additional, subvalvular procedures (such as eg, papillary muscle relocation²⁹ or approximation³⁰) appear mandatory.

Study Limitation

Clinical extrapolation from this acute, ischemic ovine open-chest model has several limitations. First, compared with our acute ischemic model, left ventricular and mitral annular dilatation as well as the mitral regurgitation grade is significantly greater in a chronic animal model or in IMR/FMR patients. It might therefore be feasible that the ring effect on left ventricular geometry in the acute model differs from chronic experimental IMR or from patients with IMR/FMR. We have, however, observed in previous ovine experiments that ventricular changes during acute

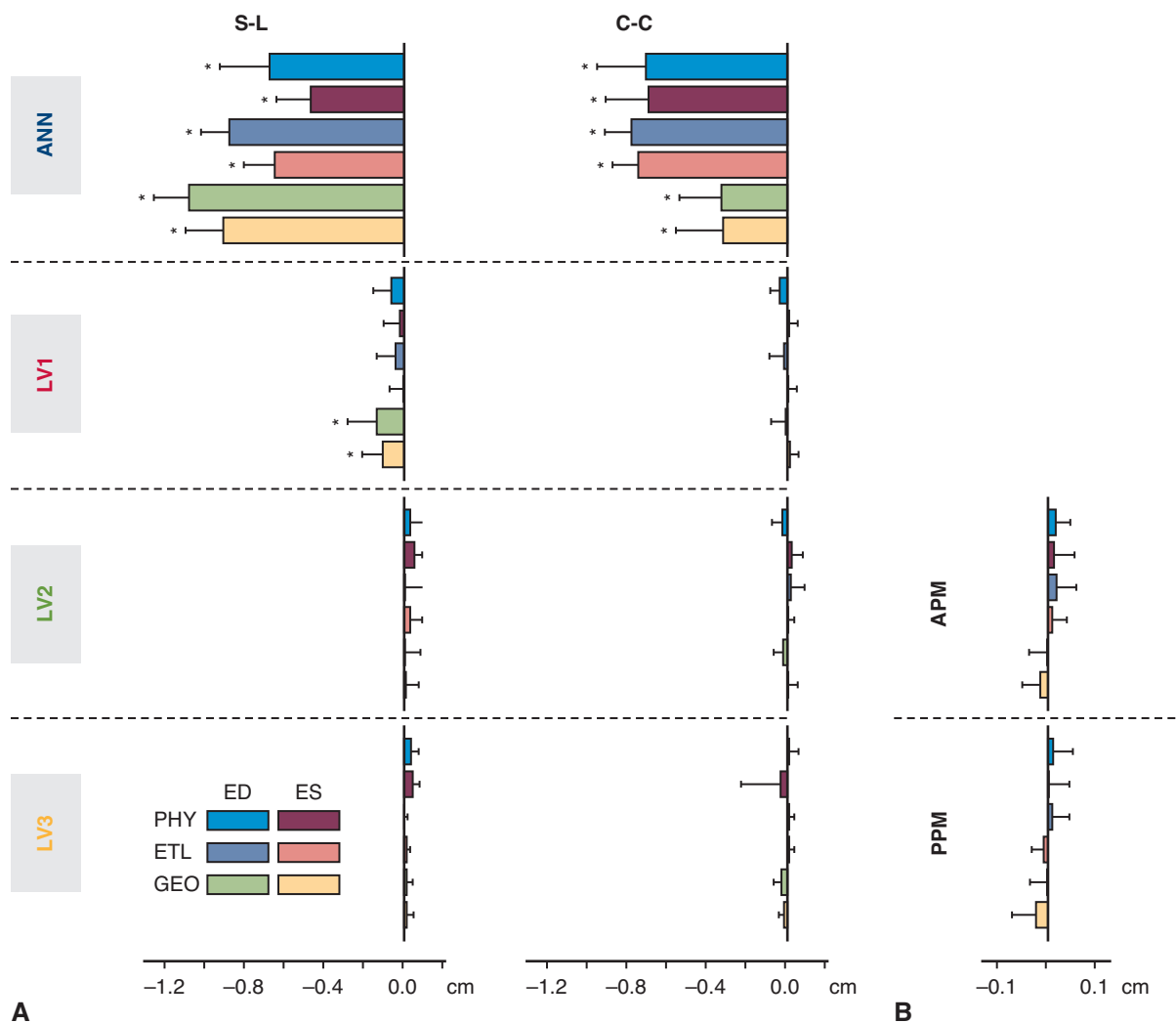


FIGURE 2. A, Mean differences (± 1 standard deviation) in septal-lateral (S-L) and commissure-commissure (C-C) diameters between NO RING versus RING on the mitral annulus (ANN), basal (LV1), equatorial (LV2), and apical (LV3) levels of the left ventricle for Physio (PHY; Edwards Lifesciences, Irvine, Calif), IMR ETlogix (ETL; Edwards Lifesciences), and GeoForm (GEO; Edwards Lifesciences) rings at end-diastole (ED) and end-systole (ES). B, Mean differences (± 1 standard deviation) in distances from the anterior and posterior papillary muscle (APM and PPM, respectively), to the left-ventricular apical plane for PHY, ETL, and GEO at ED and ES. Differences were calculated as RING minus NO RING (ie, positive or negative values reflect an increase or decrease, respectively, induced by ring implantation). Asterisks represent a statistically significant difference between NO RING versus RING according to Table 2.

myocardial ischemia are similar to those observed in the chronic setting.^{31,32} Second, our experimental approach precisely tracks distinct anatomic landmarks in all 3 dimensions and therefore includes displacements of the respective structures in any direction in 3-D space. Consequently, our results might differ from measurements obtained from clinical imaging techniques where tracking of anatomical structures is significantly more difficult. Third, true-sized PHY rings were used in our study and we cannot infer any information about the effects of downsized PHY rings. Because the GEO and ETL rings disproportionately downsize the mitral annulus in the S-L direction, we assume that the effects of downsized PHY rings are similar to those

changes observed with ETL or GEO. Fourth, no statistical comparisons between ring types were performed. However, because none of the ring types had any relevant effects on the LV or the papillary muscle geometry, such a statistical analysis appears unnecessary. Fifth, baseline was determined solely on the basis of assessing hemodynamic values (return to normal) and myocardial contraction (no regional wall motion abnormalities in the echocardiography). Neither blood samples nor myocardial tissue were harvested. Minor ischemic myocardial damage induced by LCx occlusion might therefore be possible, but major damage appears—because of the macroscopically normal cardiac performance and shortness of the ischemia time—

TABLE 3. Distances of APM and PPM to the LV apical plane at ED and ES

	Distance to LV apical plane					
	ED			ES		
	NO RING	RING	<i>P</i> value	NO RING	RING	<i>P</i> value
APM						
PHY	5.10 ± 0.77	5.12 ± 0.77	.180	4.63 ± 0.64	4.64 ± 0.63	.285
ETL	5.03 ± 0.85	5.05 ± 0.83	.142	4.56 ± 0.74	4.57 ± 0.75	.466
GEO	5.02 ± 0.47	5.01 ± 0.47	.868	4.51 ± 0.43	4.50 ± 0.41	.182
PPM						
PHY	4.14 ± 0.34	4.15 ± 0.36	.399	4.01 ± 0.33	4.01 ± 0.36	.827
ETL	4.11 ± 0.55	4.12 ± 0.54	.434	4.04 ± 0.47	4.03 ± 0.47	.476
GEO	3.99 ± 0.54	3.99 ± 0.53	.861	3.96 ± 0.52	3.93 ± 0.50	.043

All values are in centimeters, mean ± 1 standard deviation; *P* values are on the basis of a mixed effect model. Bonferroni adjusted level of significance $P < .008$. *ED*, End-diastole; *ES*, end-systole; *APM*, anterolateral papillary muscle; *PHY*, Physio annuloplasty ring (Edwards Lifesciences, Irvine, Calif); *ETL*, IMR ETlogix annuloplasty ring (Edwards Lifesciences); *GEO*, GeoForm annuloplasty ring (Edwards Lifesciences).

unlikely. Sixth, distances from both papillary muscles to a plane generated from 4 ventricular markers on the apical level (LV3) were calculated. This calculation requires that there is no change of these markers in the longitudinal position. The plane was chosen under the assumption that the markers with the largest distance to the mitral annulus are least affected by the ring implantation, but minor changes cannot be fully excluded. Seventh, our analyses were performed from data sets that have in part been published previously and the sample size was initially determined to assess differences in mitral annular and leaflet strains with and without 5 different annuloplasty rings. The possibility of different outcomes with different animal

numbers can therefore not be fully excluded. Last, our releasable ring implantation technique might have been insufficient in conforming the mitral annulus to the shape of the annuloplasty ring. Past analyses have, however, shown that the annuli conform to the ring shape in terms of S-L/C-C dimensions and height profile.^{11,15}

CONCLUSIONS

Despite radical alterations to mitral annular geometry, disease-specific IMR/FMR annuloplasty rings do not induce relevant changes to the left ventricular S-L and C-C dimensions or the geometry of the papillary muscles in the acutely ischemic ovine heart. If the findings from this acute ischemic

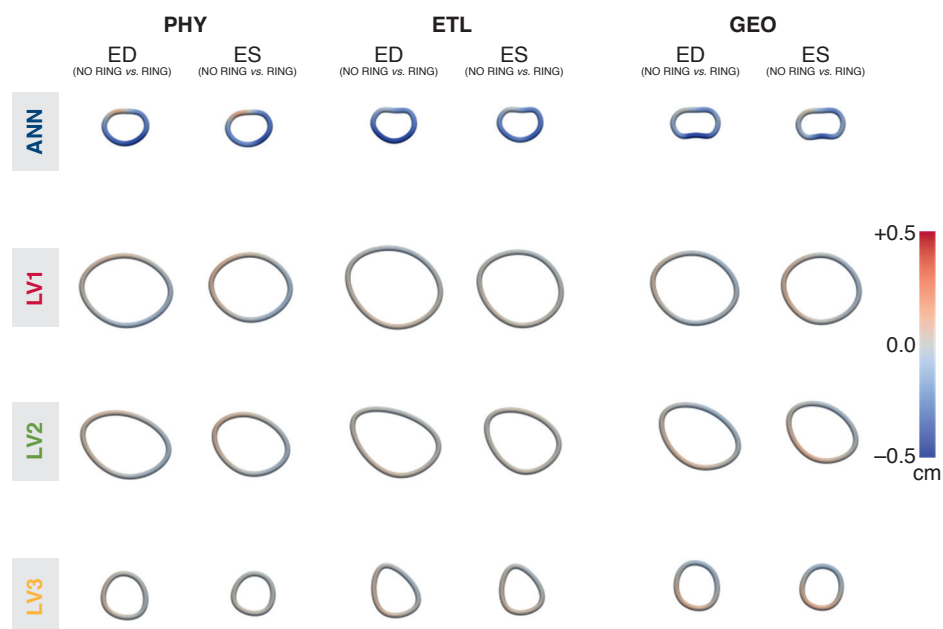


FIGURE 3. Marker-derived spline curves showing continuous transverse changes (ie, differences in distance vectors between all points on marker-generated cubic spline curves and the centers of their respective spline fits between NO RING vs. RING) of the mitral valve annulus (*ANN*) as well as basal, equatorial, and apical transverse meridians (*LV1*, *LV2*, and *LV3*, respectively) at end-diastole (*ED*) and end-systole (*ES*) for Physio (*PHY*; Edwards Lifesciences, Irvine, Calif), IMR ETlogix (*ETL*; Edwards Lifesciences), and GeoForm (*GEO*; Edwards Lifesciences) rings (see **METHODS** and **Figure 1, D**).

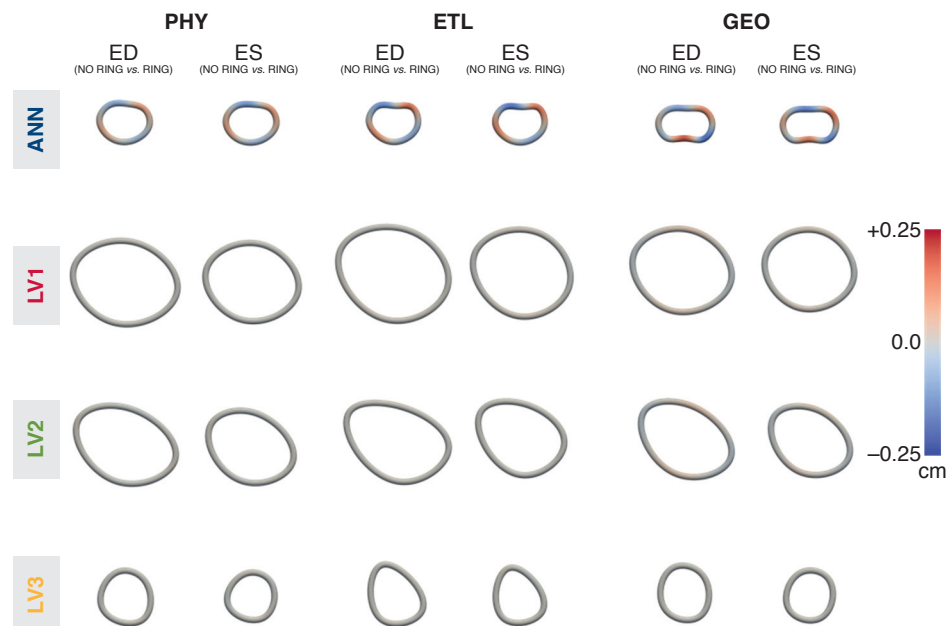


FIGURE 4. Marker-derived spline curves displaying continuous longitudinal changes (ie, differences in the normal distance of all points along the mitral annulus as well as along basal, equatorial, and apical transverse left-ventricular meridian (LV1, LV2, and LV3, respectively) from the best fit plane between NO RING vs RING) at end-diastole (ED) and end-systole (ES) for Physio (PHY; Edwards Lifesciences, Irvine, Calif), IMR ETlogix (ETL; Edwards Lifesciences) and GeoForm (GEO; Edwards Lifesciences) rings (see **METHODS** and **Figure 1, E**).

preparation do translate to patients with chronic clinical IMR/FMR, implantation of an etiology-specific designed ring alone might not be sufficient to acutely restore the ventricle to its normal elliptical shape or to reduce tethering forces induced by papillary muscle displacement.

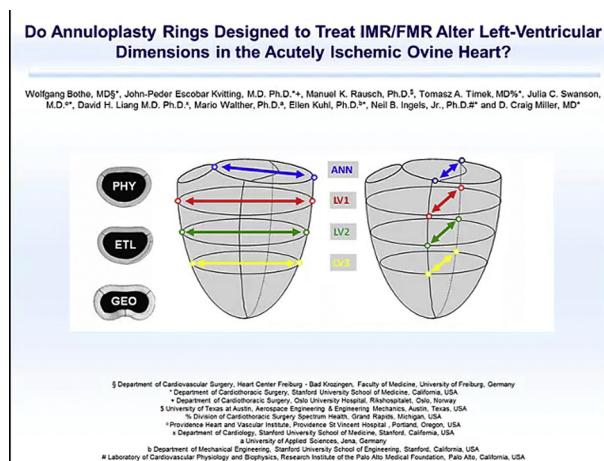
Conflict of Interest Statement

D. Craig Miller is a Consultant for Medtronic CardioVascular Division. All other authors have nothing to disclose with regard to commercial support.

The authors acknowledge the superb technical assistance provided by Maggie Brophy, Sigurd Hartnett, MD, PhD, Saideh Farahmandnia, and George T. Daughters III.

References

1. Mannaerts HF, van der Heide JA, Kamp O, Stoel MG, Twisk J, Visser CA. Early identification of left ventricular remodelling after myocardial infarction, assessed by transthoracic 3D echocardiography. *Eur Heart J*. 2004;25:680-7.
2. Jensen H, Jensen MO, Smerup MH, Ringgaard S, Sørensen TS, Andersen NT, et al. Three-dimensional assessment of papillary muscle displacement in a porcine model of ischemic mitral regurgitation. *J Thorac Cardiovasc Surg*. 2010;140:1312-8.
3. Cohn JN, Ferrari R, Sharpe N. Cardiac remodeling—concepts and clinical implications: a consensus paper from an international forum on cardiac remodeling. *J Am Coll Cardiol*. 2000;35:569-82.
4. Goldstein D, Moskowitz AJ, Gelijns AC, Ailawadi G, Parides MK, Perrault LP, et al. Two-year outcomes of surgical treatment of severe ischemic mitral regurgitation. *N Engl J Med*. 2016;374:344-53.
5. Bothe W, Swanson JC, Ingels NB, Miller DC. How much septal-lateral mitral annular reduction do you get with new ischemic/functional mitral regurgitation annuloplasty rings? *J Thorac Cardiovasc Surg*. 2010;140:117-21. 121.e1-3.
6. De Bonis M, Taramasso M, Grimaldi A, Maisano F, Calabrese MC, Verzini A, et al. The GeoForm annuloplasty ring for the surgical treatment of functional mitral regurgitation in advanced dilated cardiomyopathy. *Eur J Cardiothorac Surg*. 2011;40:488-95.
7. Votta E, Maisano F, Bolling SF, Alfieri O, Montecocchi FM, Redaelli A. The Geoform disease-specific annuloplasty system: a finite element study. *Ann Thorac Surg*. 2007;84:92-101.
8. Timek TA, Hooker RL, Collingwood R, Davis AT, Alguire CT, Willekes CL, et al. Five-year real world outcomes of GeoForm ring implantation in patients with ischemic mitral regurgitation. *J Thorac Cardiovasc Surg*. 2014;148:1951-6.
9. Bolling SF, Pagani FD, Deeb GM, Bach DS. Intermediate-term outcome of mitral reconstruction in cardiomyopathy. *J Thorac Cardiovasc Surg*. 1998;115:381-6; discussion: 387-8.
10. Bax JJ, Braun J, Somer ST, Klautz R, Holman ER, Versteegh MIM, et al. Restrictive annuloplasty and coronary revascularization in ischemic mitral regurgitation results in reverse left ventricular remodeling. *Circulation*. 2004;110(11 suppl 1): II103-8.



VIDEO 1. Presentation illustrating the key findings of this study. Video available at: [https://www.jtcvs.org/article/S0022-5223\(19\)30004-2/fulltext](https://www.jtcvs.org/article/S0022-5223(19)30004-2/fulltext).

11. Bothe W, Chang PA, Swanson JC, Itoh A, Arata K, Ingels NB, et al. Releasable annuloplasty ring insertion—a novel experimental implantation model. *Eur J Cardiothorac Surg*. 2009;36:830-2.
12. Bothe W, Kuhl E, Kvitting JP, Rausch MK, Göktepe S, Swanson JC, et al. Rigid, complete annuloplasty rings increase anterior mitral leaflet strains in the normal beating ovine heart. *Circulation*. 2011;124(11 suppl):S81-96.
13. Bothe W, Kvitting JP, Stephens EH, Swanson JC, Liang DH, Ingels NB, et al. Effects of different annuloplasty ring types on mitral leaflet tenting area during acute myocardial ischemia. *J Thorac Cardiovasc Surg*. 2011;141:345-53.
14. Bothe W, Kvitting JP, Swanson JC, Hartnett S, Ingels NB, Miller DC. Effects of different annuloplasty rings on anterior mitral leaflet dimensions. *J Thorac Cardiovasc Surg*. 2010;139:1114-22.
15. Bothe W, Rausch MK, Kvitting JP, Echtner DK, Walther M, Ingels NB, et al. How do annuloplasty rings affect mitral annular strains in the normal beating ovine heart? *Circulation*. 2012;126(11 suppl 1):S231-8.
16. Niczyporuk MA, Miller DC. Automatic tracking and digitization of multiple radiopaque myocardial markers. *Comput Biomed Res Int J*. 1991;24:129-42.
17. Daughters GT, Sanders WJ, Miller DC, Schwarzkopf A, Mead CW, Ingels J, et al. A comparison of two analytical systems for 3-D reconstruction from biplane videoradiograms; 1988. 79-82. Computers in Cardiology, 1988. Proceedings.
18. Zoghbi WA, Adams D, Bonow RO, Enriquez-Sarano M, Foster E, Grayburn PA, et al. Recommendations for noninvasive evaluation of native valvular regurgitation: a report from the American Society of Echocardiography developed in collaboration with the Society for Cardiovascular Magnetic Resonance. *J Am Soc Echocardiogr*. 2017;30:303-71.
19. Tibayan FA, Rodriguez F, Langer F, Liang D, Daughters GT, Ingels NB, et al. Undersized mitral annuloplasty alters left ventricular shape during acute ischemic mitral regurgitation. *Circulation*. 2004;110(11 suppl 1):II98-102.
20. Calafiore AM, Gallina S, Di Mauro M, Gaeta F, Iacò AL, D'Alessandro S, et al. Mitral valve procedure in dilated cardiomyopathy: repair or replacement? *Ann Thorac Surg*. 2001;71:1146-52; discussion: 1152-3.
21. Daimon M, Fukuda S, Adams DH, McCarthy PM, Gillinov AM, Carpentier A, et al. Mitral valve repair with Carpentier-McCarthy-Adams IMR ETlogix annuloplasty ring for ischemic mitral regurgitation: early echocardiographic results from a multi-center study. *Circulation*. 2006;114(1 suppl):I588-93.
22. Filsoufi F, Castillo JG, Rahmian PB, Carpentier A, Adams DH. Remodeling annuloplasty using a prosthetic ring designed for correcting type-IIb ischemic mitral regurgitation [in Spanish]. *Rev Esp Cardiol*. 2007;60:1151-8.
23. Mosquera VX, Bouzas-Mosquera A, Estévez F, Herrera JM, Campos V, Portela F, et al. Mitral valve repair for ischemic mitral regurgitation using the Carpentier-McCarthy-Adams IMR ETlogix® ring: medium-term echocardiographic findings. *Rev Esp Cardiol*. 2010;63:1200-4.
24. Gatti G, Pinamonti B, Dellangela L, Antonini-Canterin F, Benussi B, Sinagra G, et al. Mitral annuloplasty with IMR ETlogix ring for ischemic mitral regurgitation and left ventricular dysfunction. *J Heart Valve Dis*. 2012;21:556-63.
25. Martín CE, Castaño M, Gomez-Plana J, Gualis J, Comendador JM, Iglesias I. Mitral stenosis after IMR ETlogix ring annuloplasty for ischemic regurgitation. *Asian Cardiovasc Thorac Ann*. 2012;20:534-8.
26. Armen TA, Vandse R, Crestanello JA, Raman SV, Bickle KM, Nathan NS. Mechanisms of valve competency after mitral valve annuloplasty for ischaemic mitral regurgitation using the Geoform ring: insights from three-dimensional echocardiography. *Eur J Echocardiogr*. 2009;10:74-81.
27. Hernández-Vaquero D, Díaz R, Moris C. Encouraging outcomes after mitral valve repair with the GeoForm annuloplasty ring. An extraordinary ring or a very good patient selection? *J Thorac Cardiovasc Surg*. 2014;148:751.
28. Campisi S, Fuzellier JF, Haber B, Favre JP, Gerbay A, Vola M. Mid-term results of mitral valve repair for ischemic mitral regurgitation with ETlogix ring: a single-center study. *Int J Cardiol*. 2016;222:924-30.
29. Fattouch K, Castrovinci S, Murana G, Dioguardi P, Guccione F, Nasso G, et al. Papillary muscle relocation and mitral annuloplasty in ischemic mitral valve regurgitation: midterm results. *J Thorac Cardiovasc Surg*. 2014;148:1947-50.
30. Nappi F, Spadaccio C, Nenna A, Lusini M, Fraldi M, Acar C, et al. Is subvalvular repair worthwhile in severe ischemic mitral regurgitation? Subanalysis of the papillary muscle approximation trial. *J Thorac Cardiovasc Surg*. 2017;153:286-95.e2.
31. Lai DT, Timek TA, Tibayan FA, Green GR, Daughters GT, Liang D, et al. The effects of mitral annuloplasty rings on mitral valve complex 3-D geometry during acute left ventricular ischemia. *Eur J Cardiothorac Surg*. 2002;22:808-16.
32. Tibayan FA, Rodriguez F, Zasio MK, Bailey L, Liang D, Daughters GT, et al. Geometric distortions of the mitral valvular-ventricular complex in chronic ischemic mitral regurgitation. *Circulation*. 2003;108(suppl 1):II116-21.

Key Words: mitral valve, mitral regurgitation, mitral valve repair, cardiomyopathy, heart failure, pathophysiology, surgery techniques, cardiac intervention